PREDICTIONS OF THE INITIAL NON-STEADY STATE CRACK GROWTH BEHAVIOUR IN THE CREEP/FATIGUE OF THE NICKEL-BASED SUPERALLOY AP1

K M Nikbin

Department of Mechanical Engineering
Imperial College
London SW7 2BX

Abstract

Using the fracture mechanics parameters K and C* to analyse cyclic crack growth test results, carried out on a nickel-based superalloy AP1, the effects of test frequency on the initial incubation time followed by transient cracking rates and the steady state secondary crack growth rates have been considered. The cracking behaviour at 700°C for this material shows a frequency dependence over a range of 10 to 0.001 Hz. It has been shown that at high temperatures under steady state cracking conditions, fatigue processes are most dominant at high frequencies and conversely time dependant creep dominates at low frequencies. The creep cracking rate is described by a model linked to the exhaustion of available ductility in a creep process zone at the crack tip and the fatigue rate is linked to the Paris Law equation. For the secondary regime of crack growth, the effects of frequency is described in a cumulative damage model developed for creep/fatigue interaction. For the crack incubation and the transient process under initial loading the model is extended to predict the cracking behaviour in the creep regime at low cyclic frequencies. For the higher frequencies fatigue dominates and no creep transient effects are observed experimentally.

Superalloys 1992
Edited by S.D. Antolovich, R.W. Stusrud, R.A. MacKay,
D.L. Anton, T. Khan, R.D. Kissinger, D.L. Klarstrom
The Minerals, Metals & Materials Society, 1992

Introduction

Many nickel-based super alloys components in gas turbines, power plants and nuclear reactors undergo cyclic loading during their operating life at high temperatures and their permitted design tolerances against creep deformation need to be restricted due to operational and safety considerations. The mechanical and geometric constraints used in the design of these components, regardless of their creep ductility, invariably produce creep-brittle crack growth and failures in which creep damage is localised. Therefore, under plane strain conditions, it is possible to induce a crack in a material with a high uniaxial creep ductility and fatigue toughness if the crack tip damage is contained locally by means of a geometric constraint or some form of material degradation and/or testing variable. The creep/fatigue and environmental processes will thus contribute to a crack-tip controlled failures in these alloys. The dominant mode of fracture will therefore depend upon such factors as material composition, heat treatment cyclic to mean ratio, frequency and temperature and operating environment [1-3].

The applicability of linear and non-linear fracture mechanics crack growth models based on K and C* depending on the state of stress of the particular test condition at the crack-tip has become an accepted fact [2-6] for the secondary steady state stage of cracking. The initial incubation and the transient stages of cracking are still open for further analysis. Models developed for this initial behaviour are applied to tests carried out on a nickel-based superalloy (AP1) [2] (properties shown in Table 1) under cyclic loading over a range of frequencies between 0.001 Hz to 10 Hz. In this paper the transition from an elastic to a creep steady state of stress is modelled to describe the initial cyclic crack growth behaviour. The characterisation of the cracking rates in the early stage of incubation and damage accumulation upon first loading is described in terms of initial incubation time followed by the gradual increase in crack growth to coincide with the steady state cracking rate. Using the experimental data from AP1 damage due to creep and fatigue are described in terms of a cumulative damage model and then linked to a model to describe the transition phenomenon to bound the crack growth behaviour in the initial and the secondary stage of cracking.

TABLE 1 Composition and heat treatment and creep properties of Alloy AP1.

(Weight in %)							
Cr	Mo	Ti	Al	Zr	C	B	Ni
14.8	5.04	3.5	3.98	.04	.02	2e-4	Balance

Heat-treatment (AC=air Cooled)
4h 1100° C, AC, 24h 650° C, AC, 8h 760°C, AC

Creep Properties at the test temperature of 700° C.
Geometry = Compact Tension, Material properties, and failure times.

Material	n	σ_o	D	ϕ	ε_f
AP1	8	1100	5	.88	.15

where T (°C) is the test temperature, σ_o (MPa) at $\dot{\varepsilon}_o = 1/h$, n and ε_f (as a fraction) have been evaluated from rupture data, $D = D_o/\varepsilon_f^*$ is the constant in equation 3 when C* is in MJ/m^2 h and $\phi = n/n+1$.

Experimental procedure

Details of the materials and experimental procedure have been presented previously [2] and only an outline will be included here. The nickel base superalloy which was examined is designated AP1. It was received in the form of a hot isostatically pressed billet which has been heat-treated to produce a microstructure containing approximately 40 vol% of γ' phase dispersed in a γ-nickel solid solution matrix and an average grain size of 60μm. The material was tested at a temperature of 700° C, R-ratio of 0.7, frequency range of 0, and 0.001Hz to 10 Hz in the form of standard and initially pre-fatigued compact tensions of width 50mm and of two thicknesses of B=25mm and 12mm containing no side-grooves.

Modelling the cyclic crack growth behaviour

The creep/fatigue crack growth analysis for this material will need to contain two modes of behaviour. These are fatigue time-independent, and the creep time-dependant cracking modes. The fact that in the time dependant regime the cracking rate is not necessarily steady state [3,7] adds an additional variable which has to be taken into account. A model to consider all the aspects of the cracking behaviour is thus needed for use in life prediction methods and the section below describes such a model and its application to the AP1 nickel-base superalloy.

Fatigue analysis. When a cracked test piece is cyclically loaded at room temperature in the absence of any environmental conditions the cracking rate is cycle dependant and fatigue processes dominate. A fatigue threshold exists below which no crack growth can be obtained but the secondary steady state crack growth per cycle is time dependant and is given in terms of da/dN such that

$$da/dN \;\alpha\; \Delta K^m \qquad (1)$$

where da/dN is the crack growth per cycle K is the stress intensity factor and m is a material constant which has a usual value of between 2 and 4 for most engineering materials. It is also observed that at higher temperatures where cyclic loading is used equation (1) generally describes the secondary cracking behaviour of the material. Previous work on high temperature cyclic crack growth [2,3] has shown that a change of frequency effects the creep/fatigue interaction and transition points.

When the load is cycled or when temperature transients produce a cyclic loading on the structure both time independent fatigue and time dependent cracking behaviour can be observed. Generally when creep and time dependent mechanisms are involved fractures are inter granular and when cycle dependent fatigue processes dominate the failures are transgranular [2]. In the range of creep dominant cracking behaviour, at low cyclic rates, it is more appropriate [3-7] to use non-linear fracture mechanics concepts and express the steady state time dependant cracking rate $\dot{a}$ as a function of the creep fracture mechanics parameter C* [5,6] by assuming that the creep strain rate $\dot{\varepsilon}$ is governed by the Norton's creep rate

$$\dot{\varepsilon} = C\,\sigma^n \qquad (2)$$

Which gives for a cracked body [5]

$$\dot{a} = D_o\, C^{*\phi} \qquad (3)$$

or

$$da/dN = (D_o\, C^{*\phi})\,/\,f \qquad (4)$$

where $\phi = (n/n+1)$, a number slightly less than unity, and C are material constants, n is the creep index in Norton's creep law, f is the frequency, N is the number of cycles, C* is the non-linear creep parameter evaluated at maximum load, D_o is the proportionality factor determined chiefly by the material creep ductility and the constraint local to the crack tip. An increase in crack growth is obtained by an increase in the degree of constraint and with decrease in ductility. Therefore material cracking behaviour will be controlled by both the material creep properties, specimen geometry and test variables such as temperature and frequency. Equation (3) has been shown to describe time dependent cracking behaviour over a range of crack tip constraints [7] and a general model to describe creep crack growth from plane stress to plane strain is given as

$$\dot{a} = 3\, C^{*\phi} / \varepsilon_f^* \qquad (5)$$

where $\dot{a}$ is in mm/h, C* in MJ/m^2 h and the creep strain ε_f^* as a fraction. ε_f^* is taken as the material uniaxial creep ductility ε_f in plane stress and as $\varepsilon_f/50$ for the case of plane strain [8].

Generally in the low cyclic frequency range before creep redistribution occurs K describes the crack tip linear stresses but with the advance of damage with time C* will be applicable. However in the initial stages of loading and damage accumulation K and the steady state model of C* fails to describe adequately the process of crack initiation and growth. Figures 1 and 2 show a representative example of the 'tail' that exists in crack growth versus K and C* data for a the nickel based super alloy AP1, tested at various frequencies at 700°C. The initial transition tail constitutes a substantial part of test times and the modelling of this feature would improve cyclic crack growth rate predictions using the C* parameter.

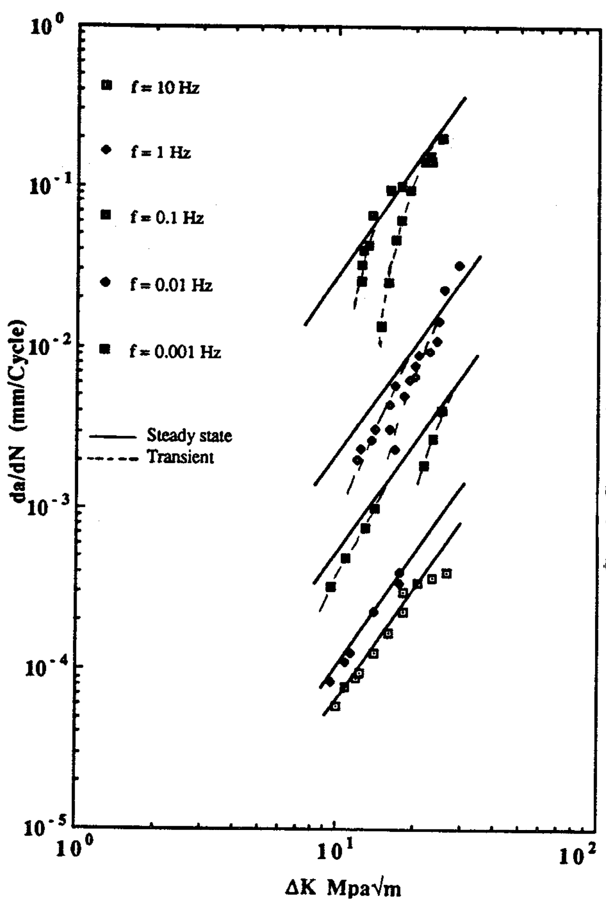

Figure 1. Example of the transient effect in the correlation of crack growth versus ΔK for AP1, CT specimens tested at 700 °C at various frequencies and R=0.7.

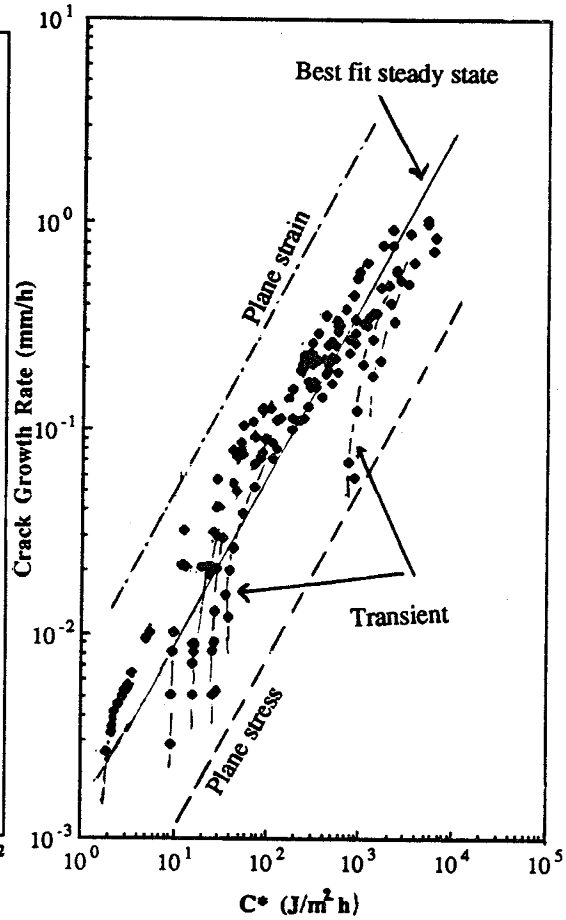

Figure 2. Example of the transient effect in the correlation of crack growth versus C* for AP1, CT specimens tested at 700 °C at various frequencies and R=0.7.

In order to predict crack growth at high temperatures a process zone (figure 3a) can be postulated at the crack tip [9] where cracking proceeds when an element of material experiences damage and rupture stressed according to the local magnified state of stress. This non-linear stress singularity determines the rate at which the element of material accumulates damage and failure occurs when the creep ductility ε_f^* appropriate to the state of stress (or to the extent of constraint) at the crack tip is exhausted. For the case of plane stress $\varepsilon_f^* = \varepsilon_f$, where ε_f is the uniaxial creep ductility, The NSW model [9] of steady state creep crack growth gives $\dot{a}_s$ in the form

$$\dot{a}_s = \{(n+1)/\varepsilon_f^*\} \left[C^*/I_n \right]^{n/(n+1)} (A\ r_c)^{1/(n+1)} \tag{6}$$

where I_n is a non-dimensional function of n, r_c is the creep process zone size over which each element sees the appropriate stress history and A is material constant. This expression assumes the development of steady state damage distribution in the region of the process zone. It assumes that zero damage exists at $r=r_c$ and that progressively more damage is accumulated as the crack tip is approached. Therefore the model assumes that little extra strain is required to break a ligament dr at the crack tip since it will be almost broken before the crack reaches it.

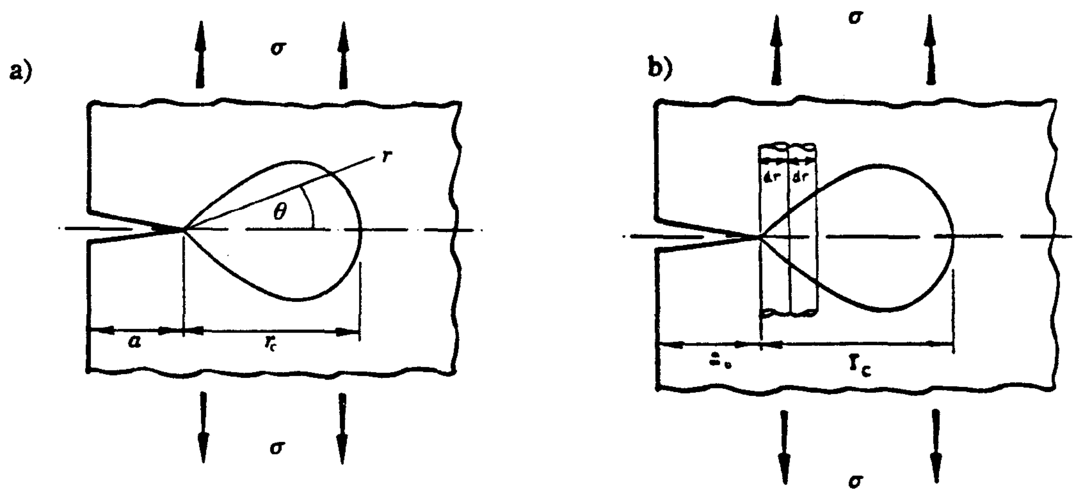

Figure 3a: Model of a creep process zone ahead of a crack tip.
3b: Ligament damage development in a creep process zone.

Transient analysis. As previously stated the experimental evidence from AP1, both in terms of K and C*, as shown in figures 1 and 2 suggests that the initial loading produces a 'tail' in the crack growth which can be attributed to a time dependant creep transition behaviour. This phenomenon has also been described mathematically in [10,11]. This transition effect would be mainly attributed to two factors. The transition time which is described as the time taken to go from an elastic state of stress at the crack tip to a steady state creep stress [7,12]. By eliminating the data points up to the point of the transition time the actual periods of the tail that have been measured are still apparent in the test data. Suggesting that upon first loading the steady state situation at the crack tip will not exist. At first loading a stable distribution of damage will need to built up ahead of the crack before steady state crack growth begins. The small ligament *dr* (Figure 1b) will not have suffered any creep strain and failure will not occur until a time dt has elapsed, given by

$$\varepsilon_f^* = \dot{\varepsilon}\ dt \tag{7}$$

where $\dot{\varepsilon}$ is the creep displacement rate. This leads to an initial creep crack growth rate $\dot{a}_o$ giving

$$\dot{a}_o = dr/dt \tag{8}$$

Giving
$$\dot{a}_o = (1/\varepsilon_f^*) \left[C^*/I_n \right]^{n/(n+1)} (A\ dr)^{1/(n+1)} \tag{9}$$

Equation (9) is very similar to that derived from the steady state damage conditions (equation (6)) . It results in the relation

$$\dot{a}_o = (1/n+1)\left(dr/r_c\right)^{1/(n+1)}\dot{a}_s \tag{10}$$

the ligament dr can be chosen to be a suitable fraction of r_c . However since dr/r_c is raised to a small power in equation (10)

$$\dot{a}_o \approx (1/n+1)\ \dot{a}_s \tag{11}$$

For most engineering materials therefore the initial crack growth rate is expected to be approximately an order of magnitude less than that predicted from the steady state analysis. The cracking rate will progressively reach the steady state cracking rate as damage is accumulated. Numerical integration is required to evaluate equation (10). A computer program has been developed, using incremental crack extension, to evaluate the transition period resulting from the development and the accumulation of damage in accordance with equations (6 and 10).

Prediction of incubation periods. Various models incorporating crack opening displacement information from tests have been developed [13-15]. This kind of data have not always been recorded and morover they are more appropriate for use in creep ductile materials. Therefore given that in most high temperature tests there is an incubation period which is attributable to the time taken for the crack to initiate to a physically measurable (only limited to the crack measuring techniques used) size, the present models of creep crack growth can then be developed to calculate an incubation period using crack length as basis for crack initiation. The model gives equations for cracking rate that are not sensitive to the process zone size since r_c in them is raised to a small fractional power. However, from microstructural observations [2] r_c can usually be taken to be about the material grain size. This size also corresponds reasonably with the limit of detection of most crack monitoring systems (50-100 μm). Consequently, in this analysis it will be assumed that crack initiation takes place when the crack has extended a distance r_c so that the incubation period t_i becomes

$$t_i = \int_o^{r_c} \frac{dr}{\dot{a}} \tag{12}$$

where $\dot{a}$ will increase from its initial transient value $\dot{a}_o$ to $\dot{a}_s$ with crack extension. A lower bound estimate of t_i can be obtained by substituting $\dot{a} = \dot{a}_s$ using equations (1), (4) and (5) to give

$$t_i = r_c / \dot{a}_s$$

$$= \left(r_c^{\,n/(n+1)}\ \varepsilon_f^*\right) / \left((n+1)\left[\ C^*/I_n\right]^{n/(n+1)}\ A^{\,1/(n+1)}\right) \tag{13}$$

Some indication of an upper bound can be determined by taking $\dot{a}$ to equal $\dot{a}_o$ from equation (9) so that

$$t_i = r_c\ \varepsilon_f^* \,/\, \left(\left[\ C^*/I_n\right]^{n/(n+1)} (A\ dr)^{1/(n+1)}\right) \tag{14}$$

Equations (13) and (14) can, therefore, be employed to provide estimates of incubation periods for crack growth from a knowledge only of uni-axial creep and stress rupture data. An estimate of the incubation period can also be obtained by using the approximate steady state creep crack growth law equation (5). If this is employed for steady state conditions, a lower bound to the incubation period in hours becomes

$$t_i \approx r_c \, \varepsilon_f^* \Big/ 3\, C^{*0.85} \tag{15}$$

with e^*_f as a fraction and C^* in MJ/m^2h. The approximate crack growth law assumes n = 5.7 to give $\phi = 0.85$. Consequently, from equation (11) if the incubation period is calculated from the initial transient cracking rate $\dot{a}_0$ determined from equation (6),

$$t_i \approx (n+1)\, r_c \, \varepsilon_f^* \Big/ 3\, C^{*0.85} \tag{16}$$

Equations (13) to (16) can then be applied to experimental data taken from creep crack growth tests. An example of the application of this model to AP1 tested at 700° C is used in the next section to relate experimental initiation times for the compact specimens tested at frequencies of less than 0.1Hz to the predictions approximated in equations (15,16).

Results. Figure 1 show the cyclic crack growth data for the whole frequency range of 10 to 0.001 Hz plotted versus ΔK and figure 2 show the low cycle crack growth data for the frequency range of 0.1 to 0.001 Hz plotted versus C*. Figure 1 shows that the effect of the transient cracking increases with the reduction in the frequency suggesting that this is a time dependant phenomena. Figure 2 shows that the effect is independent of the C* value and only occurs upon initial loading. The upper and lower bound predictions for the plane strain and plane stress cracking rates evaluated from equation (5) are also shown in the figure. The best average line drawn through the data gives an effective creep ductility at the crack tip ε^*_f=0.018 for the present AP1 data.

A sample comparison of the experimental cracking rate and the predicted rate is shown in figure 4. The predicted results show that the trends at the initial stages of the cracking rates, where a tail exists in the experimental data, are predicted by the model satisfactorily. The values of D_0 and ϕ used in equation 3 determine the accuracy with which the steady state crack growth rates are predicted. There are no visible differences. All show varying degrees of an initial tail and the model within a factor of two or less describe the transition to steady state.

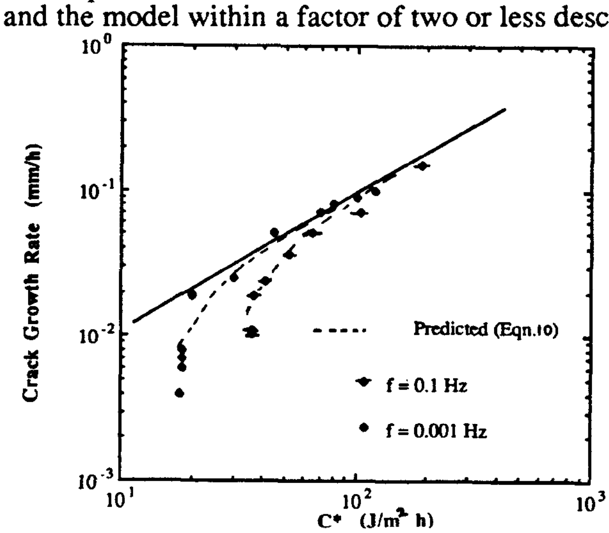

Figure 4. Sample prediction of the primary and secondary cracking rates using equation(10).

Discussion and Conclusions. It has been observed that this transition period to steady state C* is not sufficient to explain the 'tail' that exists in the low cycle creep crack growth data. Expressions developed to predict initial ligament damage accumulation at the crack tip have been applied to a nickel based superalloy.

The predicted results show that initial cracking rate $\dot{a}_0$ could be up to approximately 1/10 of the steady state crack growth rate $\dot{a}_s$. This value is consistent with the experimental data for the four alloys considered. The period over which the transition takes place in the predictions has also been found to be upto 40% of total life and it compares well with the first stage crack initiation and growth times found experimentally. Since the ideal secondary steady state does not exist in the laboratory data and primary and tertiary effects are prevalent to varying degrees the present predictions, using the ligament damage development model, show the right trends but would be dependent on the accuracy of the C* estimation procedure used.

In order to predict cyclic low frequency crack growth at high temperatures the small ligaments ahead of the crack in the process zone is assumed to behave time independently and will not have suffered any creep strain initially and failure will not occur until time has elapsed to accumulate sufficient creep strains for an increment of crack to advance. This leads to an initial crack growth rate $\dot{a}_0$ given approximately as

$$\dot{a}_0 \approx (1/n+1) \quad \dot{a}_s \tag{17}$$

where $\dot{a}_s$ is the steady state cracking rate. For most engineering materials under cyclic loading therefore the initial crack growth rate is expected to be approximately an order of magnitude less than that predicted from the steady state analysis. The cracking rate will progressively reach the steady state cracking rate as damage is accumulated.

For cyclic loading a damage accumulation model [2] gives

$$da/dN = (da/dN)_t + (da/dN)_f \tag{18}$$

where t and f refer to time and cycle dependant mode of cracking. Assuming time dependence cracking only occurs at maximum load in the cyclic tests

$$da/dN = \dot{a} / 3600f + C'\Delta K^m \tag{19}$$

where da/dN is in mm/Cycle, and $\dot{a}$ in mm/h, and C' is a material constant. This model suggests that creep and fatigue are accumulative. The frequency range of the creep fatigue interaction can thus be determined and since fatigue is time independent only the creep time dependant processes will vary the interaction range. Figure 5 shows the frequency cumulative damage model as in equation (19). The secondary cracking rate values are plotted at a constant value of ΔK=20MPa$\sqrt{m}$ versus frequency. The dashed line uses equation (17) to predict the lower bound for the creep/fatigue interaction for AP1. Since the fatigue process is independent of time all transient effects would be due to creep and the non-linear state of stress at the crack tip. The effect of the transient on the creep/fatigue range is that fatigue will be dominant at a lower frequency of below 0.01 Hz suggesting that the loading and unloading cycles could prolong the transient behaviour and the accumulation of the sufficient creep damage for the secondary state of cyclic crack growth.

The predictions for the incubation periods are shown in figure (5). The value of r_c taken is the grain size (Table 1) and equations (15,16) were used to predict the upper and lower bounds of the prediction lines. The AP1 material being a fairly creep-brittle material which shows no creep deformation of the geometry has a small ratio of incubation time in relation to the total life. Hence the figure shows for the lower, experimental C* values a shallower slope suggesting relatively smaller incubation periods as compared to the lower bound predicted lines taken from equation (15). For the higher C*

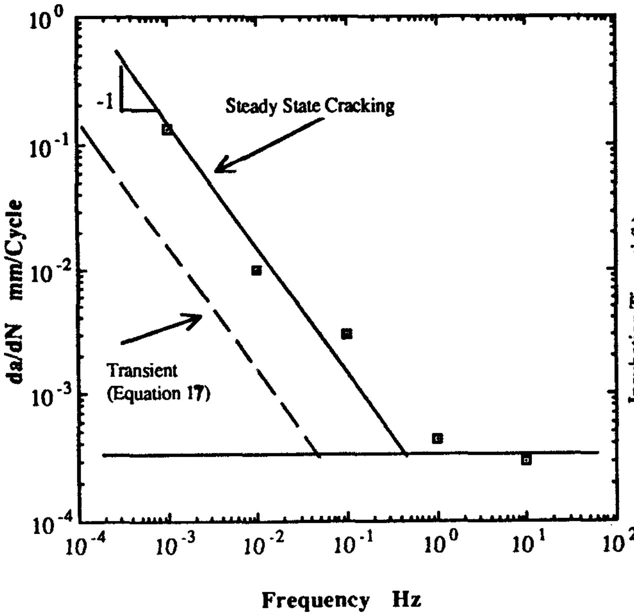

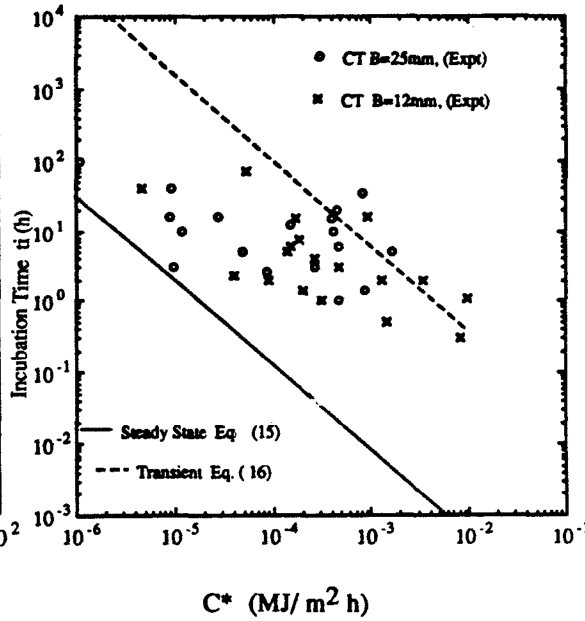

Figure 5. Frequency dependance of da/dN at ΔK=20MPa$\sqrt{m}$ for AP1 at 700° C.

Figure 6. Experimental and predicted incubation times versus C* for AP1 at 700° C.

values the incubation time are large relative to the lower bound predictions. The slowing down of the crack growth initiation may be attributed to the crack tip plasticity that occurs when a large load is applied. From figure 6 it is clear that for a safe prediction of the initiation times for the present test conditions the lowerbound line is given by

$$t_i \approx r_c \, \varepsilon_f^* / \, 3 \, C^{*0.85} \tag{20}$$

where ε_f^* is the taken as the uniaxial creep ductility $\varepsilon_f/8$ from the best fit line of the data in figure 2. Also from equation (12) it is clear that the rate of damage build up will determine the incubation time and this is dependant on the chosen value of r_c. The faster the build up of damage the closer the steady state prediction lines to data points as in figure 6 and when it develops slowly the agreement is nearer the transient prediction line. The present laboratory tests are relatively short and results from longer term tests which are more in line with component life times should be used in order to provide further support for this model.

In considering the test data for the AP1 it has been shown that the model of the creep process zone at the crack tip can be used to describe the incubation, the transient and the steady state crack growth bahaviour of this material. Approximate terms of the model, needing basic available uniaxial and crack growth data, have been put forward for use as life prediction criteria of other engineering matrials.

Acknowledgements. The author would like to thank the Defence Research Agency (Pyestock) for their financial backing of this project.

References

1. Pineau, A, "Fatigue at high temperature", Edited by R. P. Skelton , Applied Science, London, 1983.

2. Winstone, M.R., Nikbin, K.M., Webster, G.A.," Models of failure under creep/fatigue loading of a nickel-based superalloy", J. of Mat. Sci., 1985, 20, pp.2471-2476.

3. Dimopulos, V., Nikbin, K. M., Webster, G. A., " Influence of cyclic to mean load ratio on creep/fatigue crack growth", ASM Materials week '86, Lake Buena Vista, Florida, 4-9 October 1986.

4. Nikbin, K.M., Nishida, K., Webster, G.A., "Creep/Fatigue crack growth in a 10% Cr martensitic steel", ICM6 , Japan, August, 1991.

5. Nikbin, K.M., Smith, D.J., Webster, G.A.," An engineering approach to the prediction of creep crack growth", J. Eng. Mat. Tech., 1986, 108, pp.186-191.

6. Ainsworth, R.A., Goodall, I.W., "Defect assessment at elevated temperatures", J. of Press. Vessel Tech., 1983, 105, pp.263-268.

7. Nikbin, K. M., " Transition effects in creep-brittle materials", Mechanic of Creep Brittle Materials -2, Eds. A.C.F. Cocks, A.R.S. Ponter, Elsevier applied science Sept, 1991 pp. 14-24.

8. Webster, G.A., "Crack growth at high temperature", In Engineering approaches to high temperature design, eds. B. Wilshire, D.R.J. Owen, Pineridge Press,Swansea, 1983, pp. 1-56.

9. Nikbin, K.M., Smith, D.J., Webster, G.A., Influence of creep ductility and state of stress on creep crack growth, in Advances in life prediction methods at elevated temperatures, eds. D.A. Woodford, J.R. Whitehead, 1983, ASME, New York, pp. 249-258.

10. Kubo, S., Ohji, K., Ogura, K.," An analysis of creep crack propagation on the basis of the plastic singular stress field", Eng. Fract. Mech., 11, 1979, pp. 315-329.

11. Riedel, H., The extension of a macroscopic crack at elevated temperature by the growth and coalescence of microvoids, Creep in Structures, eds. A.R.S. Ponter, D.R.Hayhurst, Springer-Verlag, Berlin, 1981, pp.514-519.

12. Riedel, H., Rice, J.R., Tensile cracks in creeping solids, Fracture Mechanics, ASTM STP 700, 1980, pp.112-130.

13. Ainsworth, R.A., (1982), "The Initiation Of Creep Crack Growth," Int. J. Solids Struct., 18, 873 - 881.

14. Neate, G.J., (1986), "Creep Crack Growth In 1/2CrMoV Steel At 838 K, I: Behaviour At a Constant Load", Mater. Sci. Engng, 82, 59 - 76.

15. Piques, R., Bensussan, Ph., and Pineau, A. (1989), "Crack Initiation And Growth Under Creep And Fatigue Loading Of An Austenitic Stainless Steel", Nucl. Eng. and Design, 116, 293 - 306.